Genomics 118 (2026) 111230

Contents lists available at ScienceDirect

Genomics

journal homepage: www.elsevier.com/locate/ygeno

Research Paper

Integration of ATAC-seq and RNA-seq unravels chromatin accessibility associated with gonad development after sex reversal in *GIFT tilapia*

Ye Yuan [a,1], Hongbo Xi [a,1], Shandong Chen [a], Zexun Zhou [a], Wenting Zhu [a], Yunyun Liu [a], Yongchun Li [a], Zhongyuan Shen [a,b,c], Chongqing Wang [a,b,c], Jun Xiao [a], Shi Wang [a,*], Wuhui Li [a,b,c,*], Shaojun Liu [a,*]

[a] *Engineering Research Center of Polyploid Fish Reproduction and Breeding of the State Education Ministry, College of Life Sciences, Hunan Normal University, Changsha 410081, China*
[b] *Hunan Yuelu Mountain Scienece and Technology Co.Ltd. Amid at Aquatic Breeding, Changsha 410081, China*
[c] *Hunan Buckwheat Lake High Quality Fish Research Institute Co., Ltd, Yueyang 414499, China*

ARTICLE INFO

Keywords:
Chromatin accessibility
Sex reversal
Transcription factor
GIFT tilapia
Gonadal development

ABSTRACT

The epigenetic mechanisms regulating gonadal development and maintenance in fish following hormone-induced sex reversal remain poorly understood. In order to address this knowledge gap, an integrated multi-omics analysis was conducted in *GIFT tilapia*. The present study compared three distinct groups: normal females (CF; genetically female, XX), normal males (CM; genetically male, XY), and pseudo-females (S; estrogen-treated genetically males, XY). The S group demonstrated intermediate growth traits and sex hormone levels that fell between those observed in the CF and CM groups. In comparison with the CF group, the S group exhibited delayed development, characterized by diminished ovarian volume, reduced oocyte numbers, and diminished oocyte quality. ATAC-seq analysis revealed unique patterns of chromatin accessibility in pseudo-female gonads, thus identifying key transcription factors, including ZNF148, ZNF281, and SP9. Integration of chromatin accessibility changes with transcriptional reprogramming has been shown to result in the identification of co-regulated genes that are enriched in critical pathways, including binding and catalytic activities, apoptosis, metabolism, and homologous recombination. Subsequent analysis identified several genes associated with gonadal development, including *ncoa4* and *gdf9*. It is noteworthy that *ncoa4* emerged as a potential core hub gene whose expression correlates with the enrichment of ZNF148/SP9 motifs and alterations in chromatin accessibility. This gene may interact with other factors, such as *esr2*, to potentially influence oocyte development. These findings may provide new insights into the epigenetic and transcriptional regulatory mechanisms associated with gonadal development following sex reversal, thereby laying a theoretical foundation for the optimization of sex control strategies in aquaculture.

1. Introduction

In nature, the growth rates between female and male populations in many fishes are different. For example, female fish exhibit a faster growth rate than males in species such as topmouth culter (*Culter alburnus*), Japanese flounder (*Paralichthys olivaceus*), yellow drum (*Nibea albiflora*), and rainbow trout (*Oncorhynchus mykiss*). In contrast, the opposite pattern is observed in yellow catfish (*Pelteobagrus fulvidraco*), Nile tilapia (*Oreochromis niloticus*), and hook snout carp (*Opsariichthys bidens*), where males grow faster than females [1–3]. In aquaculture, the difference in growth rates between male and female fish is one of the important factors affecting the aquaculture benefits. Therefore, it is of great significance to breed fish species with all- male or all-female fish strains. Recently, diet supplement with exogenous hormone (including 17β-estradiol and 17 α-methyltestosterone) has become an effective method for inducing sex differentiation [4,5].

Sex differentiation in fish is defined as the process by which primordial gonads develop into either female or male gonads during the embryonic or larval stages. The process is initiated from primordial germ cells (PGCs). As the fish embryo develops, PGCs migrate and settle,

* Corresponding authors.
E-mail addresses: wangshixyz@126.com (S. Wang), liwuhui11@163.com (W. Li), lsj@hunnu.edu.cn (S. Liu).
[1] These authors have contributed equally to this work.

https://doi.org/10.1016/j.ygeno.2026.111230
Received 16 November 2025; Received in revised form 4 March 2026; Accepted 7 March 2026
Available online 9 March 2026
0888-7543/© 2026 Published by Elsevier Inc. This is an open access article under the CC BY-NC-ND license (http://creativecommons.org/licenses/by-nc-nd/4.0/).

differentiating into spermatogonial or oogonial stem cells, which ultimately develop into functional sperm or eggs [6]. Sex differentiation and gonad development are influenced by genetics (sex-determining genes), endocrine regulation, and environmental factors, and exhibit high diversity and plasticity. For instance, the *sox9* and *amhy* pathways that govern testis development are initiated and activated in XY-type fish such as largemouth bass (*Micropterus salmoides*) and South American cichlids (*Astyanax altiparanae*) and simultaneously suppress the expression of genes involved in ovary development (e.g., *foxl2*) [7–9]. The above process serves to guide germline stem cells toward a differentiation process known as spermatogonial differentiation. In contrast, in some primarily genetic sex determination (GSD) species that exhibit temperature-sensitive sex reversal, such as Nile tilapia (*Oreochromis niloticus*) and medaka (*Oryzias latipes*), incubation temperature has been shown to modulate the differentiation direction of germline stem cells by regulating gonadal androgen (e.g., testosterone) and estrogen (e.g., estradiol) levels [10,11]. Despite the extensive research that has been conducted on exogenous hormone-induced sex differentiation in fish, studies on gonadal development maintenance after sex reversal and its underlying molecular regulatory mechanisms remain scarce.

While extensive research has been conducted on exogenous hormone-induced sex differentiation in fish, the majority of existing work has focused on the initiation of sex reversal and the expression dynamics of critical sex-determining genes during hormone administration. However, following the cessation of hormone treatment, the molecular mechanisms—particularly epigenetic ones—responsible for sustaining the long-term stability of the reversed gonadal phenotype are still poorly understood. This lack of knowledge constrains a fuller understanding of how gonads in sex-reversed individuals maintain stability and develop normally. Therefore, investigating the transcriptional regulatory mechanisms governing gonadal development after sex reversal is of paramount importance. The ATAC-seq (Assay for Transposase-Accessible Chromatin using sequencing) technique enables genome-wide detection of open chromatin regions, allowing the identification of cis-regulatory elements (e.g., promoters, enhancers) and providing insights into how transcription factors coordinate and regulate gonadal development in pseudo-females [12]. Therefore, to systematically explore the potential regulatory mechanisms underlying gonadal development in pseudo-female GIFT tilapia following EE2-induced sex reversal, this study integrated histological analysis, ELISA, RNA-seq, and ATAC-seq approaches. It aimed to uncover the dynamic relationship between chromatin accessibility patterns and gene expression levels during ovarian maturation in pseudo-females and to elucidate the associated regulatory network. These findings will provide fundamental data for the tilapia aquaculture industry.

2. Materials and methods

2.1. Ethics statement

All the experimental procedures were conducted following the standards and ethical guidelines established by the Animal Ethical Review Committee of Hunan Normal University, Changsha, China.

2.2. Animals and sample collection

GIFT tilapia broodstock were purchased from the Nanning Tilapia Hatchery in Nanning, Guangxi, China, and reared at the Hunan Buckwheat Lake High Quality Fish Research Institute Co., Ltd., Yue yang, Hunan, China. A total of 1000 larval fish (after the yolk sac was absorbed) were randomly selected and divided into two pools ($n = 500$, 3 m × 2 m = 6 m^2). The fish in each pool were artificially fed three times a day (at 8:30, 12:30, and 16:30) for 30 days. The experimental group was fed a basal diet containing 100 mg/kg of 17α-ethynylestradiol (Purity ≥98%, CAS—No. 57–63-6, SGWALDRICH, Co.) [13], while the control group received standard basal feed. After 30 days of hormone treatment, both groups were switched to the basal feed diet. Throughout the experiment, the pH of the water was maintained at 7.5–8.0, the concentration of dissolved oxygen remained above 5.0 mg/L and the temperature of the water was controlled at 23.0–27.0 °C.

The genotypes (XX/XY) of fish in both experimental and control groups were determined using sex-specific SCAR5 markers (forward primer: 5′-TTCCTCAGGGATCTGTCCTTGGT-3′; reverse primer: 5′-CAGAAATGTAGACGCCCAGGTATC-3′) [14]. Histological experiments and gonadal developmental stage assessments were conducted according to established methodologies [15]. Based on genotype and gonadal histology, the fish were categorized into three groups: the normal male group (CM), untreated genetic males (XY); the normal female group (CF), untreated genetic females (XX); and the pseudo-female group (S), genetic males (XY) that underwent EE2-induced sex reversal. Six-month-old fish were randomly selected from the CM, CF and S groups($n = 9$) and euthanized using MS222 (Purity ≥98%, E10521, Sigma-Aldrich) anesthesia for 15 min. Gonadal samples were collected and immediately frozen in liquid nitrogen before being transferred to −80 °C storage for subsequent analysis.

The body weight, gonads, and viscera of each group ($n = 10$) of Tilapia were weighed using an analytical balance, and the average body weight, gonad weight, and viscera weight for each group were recorded. The calculation of the following physiological indices was to be undertaken, with the data for this purpose to be derived from the weighing data:

$$\text{Gonadosomatic index (GSI)} = \text{Gonad weight/body weight}^{*}100$$

$$\text{Viscerosomatic index (VSI)} = \text{Total visceral weight/body weight}^{*}100$$

2.3. Estrogen/androgen testing

Blood samples were collected from one-year-old tilapia (CM, CF, S group, $n = 9$) via the caudal vein and immediately mixed with an equal volume of ACD anticoagulant (ACD, NO. B541008, Sangon Biotech). The mixed blood samples were then subjected to centrifugation in order to separate and collect the serum. In accordance with the protocol stipulated in the fish-specific estrogen/androgen ELISA kit (E ELISA Kit, ml003454; 11-KT ELISA Kit ml538868B; mlbio, Shanghai, China) manual, the respective hormone levels in the serum were quantitatively analyzed. The enzyme-linked immunosorbent assay (ELISA) reader (Bio Tek, USA.) was used to quantitate the optical density (OD) values at 450 nm for each reaction well. Concentrations of estradiol and 11-KT in the serum samples from each group of Tilapia were calculated based on the standard curve. All samples were analyzed in triplicate.

2.4. ATAC-seq

For ATAC-seq analysis, gonadal tissues were collected from three randomly selected fish ($n = 3$) from each of the CM, CF, and S groups at six months of age for library construction and sequencing. First, the preparation of a cell suspension should be undertaken, with the subsequent release of nuclear chromosomes and nucleic acids being achieved through the process of lysis [16]. Subsequently, the resulting nucleic acid suspension should be added to a transposase-containing transposition reaction mixture and incubated at 37 °C for 30 min, the products were purified with a MiniElute DNA Kit (Qiagen, Hilden, Germany). Subsequent to the process of incubation, the purified fragmented DNA functions as the template for PCR amplification, with the objective of constructing ATAC-seq-specific DNA libraries, and sequenced using an Illumina HiSeqTM 4000 by Beijing Biomarker Technologies Co. (Beijing, China). Sequencing results were analyzed on the BMKCloud platform (www.biocloud.net).

2.4.1. Sequenced reads processing

Raw sequencing reads were processed to remove adapter sequences and low-quality bases using Cutadapt. Reads shorter than 35 bp, containing more than 10% undetermined bases (N), or with over 50% of bases having a Phred quality score (Q) ≤ 10 was discarded. The resulting high-quality clean reads were used for all downstream analyses.

2.4.2. Read alignment

Using the bowtie2 (version 2.2.4, Baltimore, MD, USA) software, the high-quality reads obtained from sequencing each sample were aligned against the reference genome (https://ftp.ncbi.nlm.nih.gov/genomes/all/GCF/001/858/045/GCF_001858045.2_O_niloticus_UMD_NMBU/).

2.4.3. Peak scanning

MACS2 (version 2.2.7.1, Boston, MA, USA) was used for peak calling and estimate the empirical false discovery rate (FDR). Finally, FDR < 0.05 was selected as the identified peak.

2.4.4. Functional annotation and analysis of genome-wide peak

The ChIP seeker package (version v1.16.1, Guangzhou, China) was used for functional annotation of genome-wide Peaks. By means of BLAST, the genes associated with the peak regions were aligned against the NR, Swiss-Prot, GO, and KEGG functional databases to obtain their annotations for gene function analysis. The R package cluster Profiler was performed to analyze GO, KEGG pathway enrichment for Peak region-associated genes enriched in the Promoter region.

2.4.5. Motif analysis

MEME-ChIP 4.11.2 was used to identify and annotate Motif. Using Tomtom to align the detected Motif sequence with a known Motif.

2.4.6. Difference peak analysis

For studies with biological replicates, differential accessibility analysis was performed between two conditions/groups using the DESeq R package (version 1.6.3). The differential screening criteria are: fold change ≥2 and FDR ≤ 0.01.

2.5. RNA-seq

The present study was performed transcriptome sequencing on the S, CM and CF groups ($n = 9$) at six months of age. The total RNA of the gonad samples was extracted using TRIzol reagent (Invitrogen, USA) in a standard experimental protocol. The differential expression genes (DEGs) were identified using the DESeq2 (version 2.13) with screening thresholds of a false discovery rate (FDR) < 0.01 and an absolute Fold Change (FC) ≥ 2. The resulting data has been cleaned and uploaded to the NCBI Sequence Read Archive (SRA) database (accession number PRJNA1206816) [17].

2.6. Validation by qPCR

Total RNA was extracted following the protocol detailed in Section 2.5. QPCR (NO. A28139, Applied Biosystems)-detected transcriptome data for genes associated with gonadal development were analyzed to determine whether their expression profiles were similar to those inferred from RNA-seq data. The relative expression of genes was calculated using the $2^{-\Delta\Delta Ct}$ method, and β–actin served as an internal reference gene. Experimental protocol was performed as described in previous studies [18].

2.7. Statistical analysis

Data are presented as mean ± standard error of the mean (SEM). Differences among the three groups (CF, CM, S) were analyzed using one-way analysis of variance (ANOVA) followed by Tukey's honest significant difference (HSD) post hoc test for multiple comparisons, using SPSS 22.0. Differences between two groups were analyzed using Student's *t*-test. $P < 0.05$ was considered statistically significant.

3. Results

3.1. The growth level and gonad development of experiments fish

The results of the PCR amplification using the SCAR5 primers are shown in Fig. S1, yielding band sizes consistent with those reported in the Sun paper. Histological analysis of gonadal tissue from 20 randomly selected XY-type tilapia revealed that approximately 60% of XY-genotype individuals in the experimental group were female [17]. An analysis was conducted to assess the growth performance of the experimental fish. The results are presented in Table 1. The BW of the S group demonstrated no significant difference when compared to the control group (CF); however, it was found to be significantly lower than that of the male CM group ($p < 0.05$). Concurrently, the S group's GW and GSI exhibited no substantial discrepancy from male CM; however, they were notably lower than those observed in the CF group. The S group's TVW exhibited no significant difference from CM, yet was considerably higher than CF. Furthermore, the S group's VSI exhibited a marked increase in comparison to both parental lines.

At six months of age, the testes of CM fish contained abundant spermatids (ST), a small number of spermatogonia (SG), and spermatozoa (SZ) (Fig. 1A). At 12 months of age, the testes were found to contain numerous spermatids and spermatozoa, along with a small number of spermatocytes (SC) (Fig. 1B). At six months of age, ovarian tissues from the CF groups contained abundant stage I, II and III oocytes and the S groups contained abundant stage I, II oocytes (Fig. 1C and E). At 12 months, the ovaries of the CF group predominantly contained stage V oocytes (Fig. 1D), while those of the S group contained oocytes at various developmental stages, including stages III, IV, and V (Fig. 1F). Histological analysis revealed that at six months of age, the development of oocytes in the S group (pseudo-females) lagged behind that in the CF group (normal females). By twelve months of age, this developmental retardation became more pronounced: at equivalent body weights, ovaries in the S group were significantly smaller than those in the CF group and displayed insufficient yolk deposition, whereas ovaries in the CF group were fully developed with abundant yolk accumulation. (Fig. S2).

3.2. Hormone content testing

The estradiol (E2) and 11-KT levels in tilapia were determined using the Fish Estrogen/Androgen Detection Kit (Fig. 2). With regard to the detection of estrogen, the E2 levels in the sex-reversal group (S group) were found to be intermediate between those of the normal male group (CM) and the normal female group (CF). However, these levels were found to be significantly higher than those in the CM group ($p < 0.05$). No statistically significant difference was observed in comparison to the CF group. In androgen testing, the CF group exhibited significantly lower 11-KT levels than normal male fish, while the S group showed markedly higher 11-KT levels than normal female fish ($p < 0.05$), though still lower than normal male fish. The results indicate that

Table 1
The body weight and growth index of the three groups fish.*

	BW	GW	TVW	GSI	VSI
CF	467.69 ± 23.56^{a}	5.68 ± 1.56^{b}	18.92 ± 2.28^{b}	2.09 ± 0.43^{b}	7.05 ± 0.28^{b}
CM	535.61 ± 19.71^{b}	0.57 ± 0.04^{a}	22.27 ± 2.34^{a}	0.17 ± 0.01^{a}	6.62 ± 0.34^{b}
S	481.60 ± 20.12^{a}	1.09 ± 0.36^{a}	24.78 ± 3.57^{a}	0.38 ± 0.09^{a}	8.76 ± 0.78^{a}

* Different letters indicated significant different in the three groups fish ($p < 0.05$, ANOVA analysis).

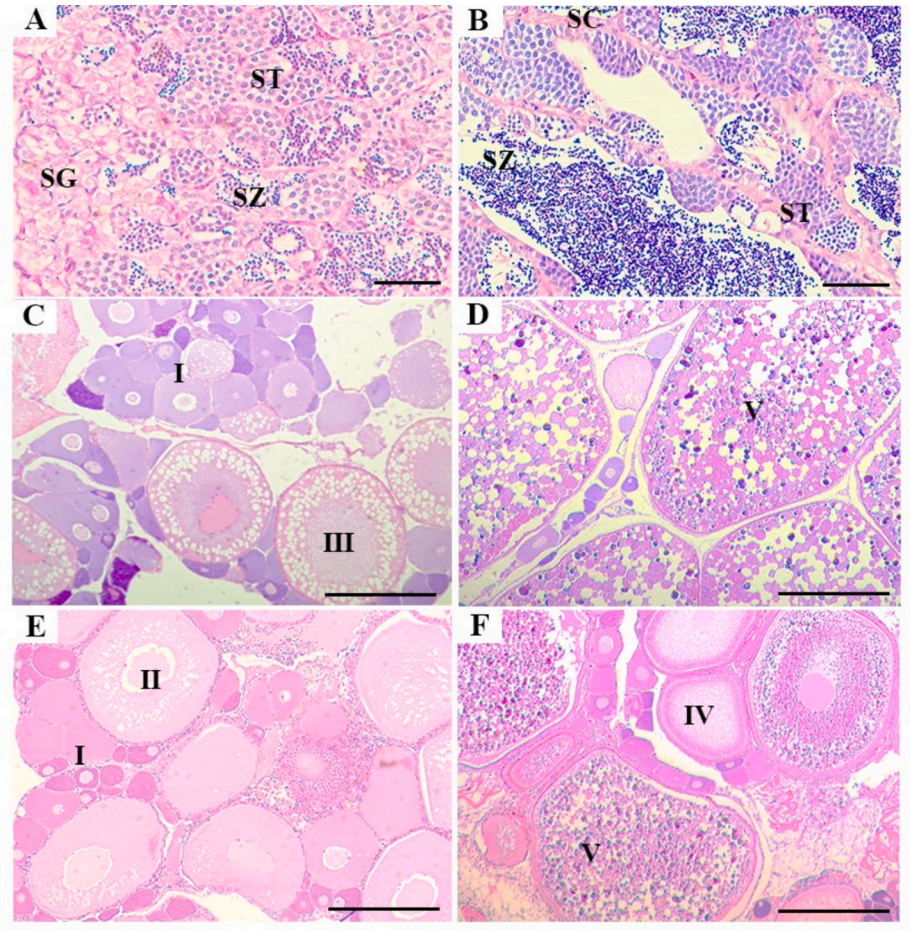


Fig. 1. The microstructure of testis and ovary in the three groups fish at different development stage.
A and B: shows the microstructure of CM fish in 6 and 12-months old, respectively; C and D: shows the microstructure of CF fish in 6 and 12-months old, respectively; E and F: shows the microstructure of S fish in 6 and 12-months old, respectively. A and B: bar = 200 μm, C-F: bar = 500 μm. SG, spermatogonia; SC, spermatocytes; ST, spermatids; SZ, spermatozoon. I: primary growth perinuclear; II: primary growth cortical alveoli; III: early vitellogenesis; IV: vitellogenesis; V: maturation.

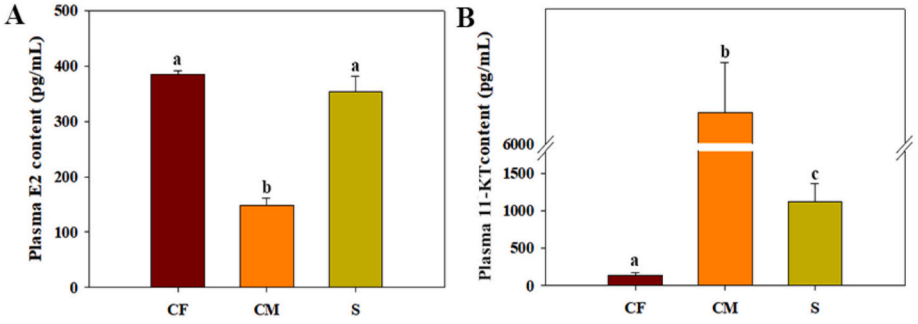


Fig. 2. Estrogen/Androgen Content in Three Groups of Fish at the One-Year-Old Stage.
A: The hormone content of E2 in the three fish species; B: The hormone content of 11-KT in the three fish species.

pseudo-females exhibit significant alterations in both estrogen and androgen secretion. The endocrine status of pseudo-females differs from both normal males and normal females.

3.3. *Application of ATAC-seq in the gonads of Tilapia*

The evaluation of the sequencing results is documented in Table S1, while the reference genome alignment results are presented in Table S2. All libraries yielded fragment lengths with expected distributions. The analysis revealed the presence of a predominance of short fragments (less than 200 base pairs, representing open chromatin between nucleosomes) and the inclusion of larger fragments (a minimum of 200 base pairs, representing open chromatin spanning nucleosomes) in decreasing abundance with increasing length (Fig. S3). The potential presence of open chromatin regions was detected across all sample groups. The number of peaks detected in each group is detailed in Table S3. The detected ATAC-seq signals were analyzed within the gene body region (The region spanning from the transcription start sites (TSS) to the Transcription End Site (TES)) (Fig. S4). Approximately 20% of the putatively accessible regions detected by ATAC-seq are located within 2 kilobases (kb) upstream of TSS, particularly within the 1-kb upstream promoter region. Approximately 30% of these genes are located in distal

intergenic regions, while the remaining 55% are found within introns, exons, and downstream of genes. Accessible regions identified by ATAC-seq were predominantly enriched within a 1.5-kilobase range around TSS (Fig. 3A). Principal component analysis (PCA) was performed (Fig. 3B). The S group did not demonstrate a complete shift toward CM and CF. Differential analysis of ATAC-seq and RNA-seq data was conducted, with significance thresholds set at a fold change $\geq$2 and an FDR (False Discovery Rate) $\leq$ 0.01. A total of 185 DARs were detected in the CF vs. S group, comprising 93 regions that were found to be up-regulated and 92 regions that were found to be down-regulated. In the CM vs S group, 771 DARs were identified, including 542 regions that were found to be up-expressed and 229 regions that were found to be down-expressed (Fig. 3C). In the RNA-seq analysis, DEGs revealed 5535 genes that were found to be up-expressed and 5220 genes that were found to be down-expressed in the CM compared to the S group, while 1284 genes were up-expressed and 552 were down-expressed in the CF compared to the S group (Table S4). In order to identify potential drivers of differences in chromatin accessibility, a screen was conducted for enriched transcription factor (TF) motifs across groups (Fig. 3D). In the CM vs S group, significant enrichment was observed for the following motifs: PATZ1, SP9, ZNF148, and ZNF281. The presence of additional enriched transcription factor motifs, including PHOL and PRDM9, was observed in this group. A comparison of the CM group with the S group revealed the presence of motifs such as ZNF384, Spi1, EWSR1-FLI1, and ERF::FOXO1, which were not detected in pseudo-female fish. Furthermore, in the comparison between the CF and S groups, only the RXRB and Nr1H2 genes demonstrated enrichment, while no other transcription factor motifs exhibited significant enrichment. Motif enrichment analysis further revealed that ZNF189, TFAP4::ETV1, ETV5::FLGLA, and CTCF showed no enrichment when comparing the CM group to the S group.

3.4. ATAC-seq and RNA-seq co-analysis

Clustering heatmap analysis of ATAC chromatin accessibility and RNA gene expression levels were performed for all samples (Fig. 4A). The results obtained from this study indicate that the chromatin open regions observed in the S group did not fully match the characteristics of either the normal female group or the normal male group in terms of gene expression levels. Following sex reversal, widespread chromatin accessibility was observed alongside gene expression reprogramming. Following the integrated analysis of chromatin accessibility (ATAC-seq) and transcriptomic (RNA-seq) data, we systematically compared the differential accessible regions (DARs) and differentially expressed genes (DEGs) between the CM and S groups. The integrated analysis identified 115 genes that were upregulated in both datasets (Fig. 4B). Further correlation analysis revealed that there were very few genes with significant DAR-DEG associations between the CF and S groups, indicating that the epigenetic landscape of pseudo-females (S) closely resembles that of natural females (CF). In sharp contrast, a large number of significant DAR-DEG associations were observed between the CM and S groups, and these associations were predominantly characterized by a positive regulatory pattern, where increased chromatin accessibility (DAR-Gain) was accompanied by upregulated gene expression (Table S5). Based on this pattern, subsequent research will focus on an in-depth analysis of the gene set exhibiting both DAR-Gain and DEG-up in the CM vs. S comparison. GO functional enrichment analysis (Fig. 4C) showed that, in terms of molecular function, the screened genes were predominantly characterized by binding and catalytic activities, such as ribosomal large subunit binding, mRNA binding and ribonucleoprotein

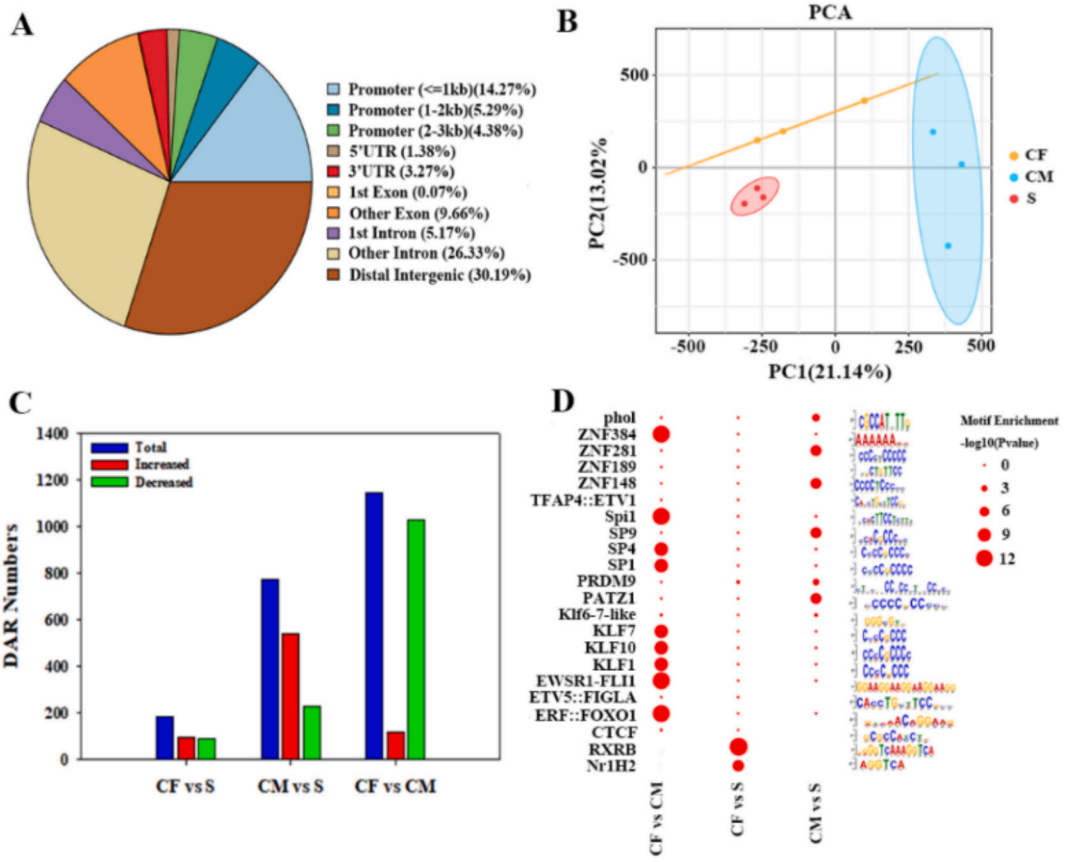


Fig. 3. Distribution, Clustering and Motif Enrichment of Differential Chromatin Accessibility.
A: Proportion of ATAC-seq peaks in various genomic annotation regions; B: PCA analysis of peak; C: Analysis of DARs in Different Groups; D: Enriched motifs and DNA sequences across different groups.

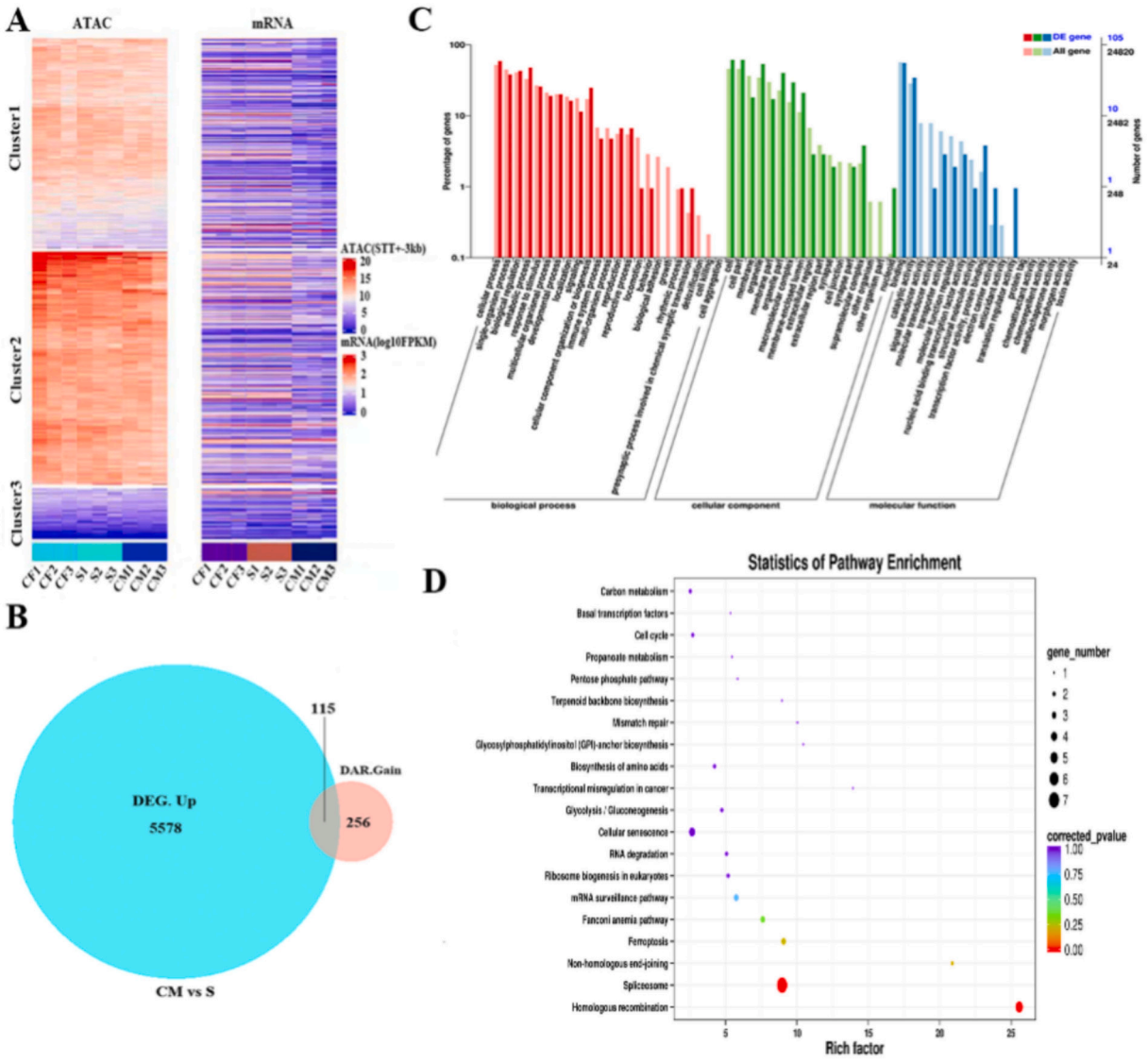


Fig. 4. Integrated ATAC-seq and RNA-seq Analysis.
A: ATAC-Seq and RNA-Seq Complex Heat map Clustering Analysis ; B: DAR genes and DEGs are co-upregulated in CM vs S; C: GO Annotations of DEGs in CM vs S; D: KEGG Pathway Enrichment Analysis of DEGs in CM vs S.

complex binding. In the biological process category, the DNA biosynthetic process and mRNA splicing, via spliceosome were significantly enriched. KEGG pathway enrichment analysis (Fig. 4D) further revealed that the homologous recombination and spliceosome-related pathways exhibited significantly enriched, whereas the pathways involved in cellular senescence and amino acid biosynthesis were associated with a larger number of differentially expressed genes.

A comprehensive analysis was performed on the transcription factor (TF) enrichment patterns and differentially expressed genes between the CM group and the S group. The results demonstrated that multiple transcription factors were significantly enriched in both datasets, including ZNF148, PRDM9, ZNF281, SP9 and PATZ1 (Table S6). An analysis was subsequently conducted on the potential transcriptional regulators inferred to affect gonadal development after sex reversal (Fig. 5A). The findings revealed that nuclear receptor coactivator 4 (*ncoa4*) was a key hub gene within this transcriptional regulatory network. *Ncoa4* exhibited significantly upregulated expression in the S group and was positively correlated with the expression of ZNF148, ZNF281 and SP9; this discovery was highly associated with the enhanced chromatin accessibility. Meanwhile, multiple genes involved in biological processes such as sex determination, steroid synthesis and cell proliferation showed differential expression patterns, including *esr2*, *cyp17*, *bmp6*, *tgfb2*, *tesk1* and *gdf9*. These genes were closely related to testicular or ovarian development and displayed co-expression correlation with ZNF148. In addition, the expression levels of several other genes (e.g., *csk*, *fgfr2*, *csflr*) were correlated with that of *ncoa4*; the expression patterns of *ficd*, *parl*, *paip2b* and *chtf8* also indicated associations with these transcription factors. Collectively, these correlations constitute a sophisticated transcriptional regulatory network.

3.5. qPCR validation

Among the differentially expressed genes identified, 13 genes were selected for qPCR validation to assess the reliability of the RNA data (Table S7). qPCR analysis was performed using six biological replicates ($n = 6$), and the results indicated that the expression patterns of these genes were largely consistent with the transcriptome data (Fig. 6). In pseudo-female gonads, *gdf9*, *mos*, *wnt4*, *ncoa4*, and *tesk1* were significantly upregulated ($p < 0.05$), while *ers2*, *bmp6*, *foxo3*, *gsdf*, *fgfr2*, and *rarg* were significantly downregulated ($p < 0.05$).

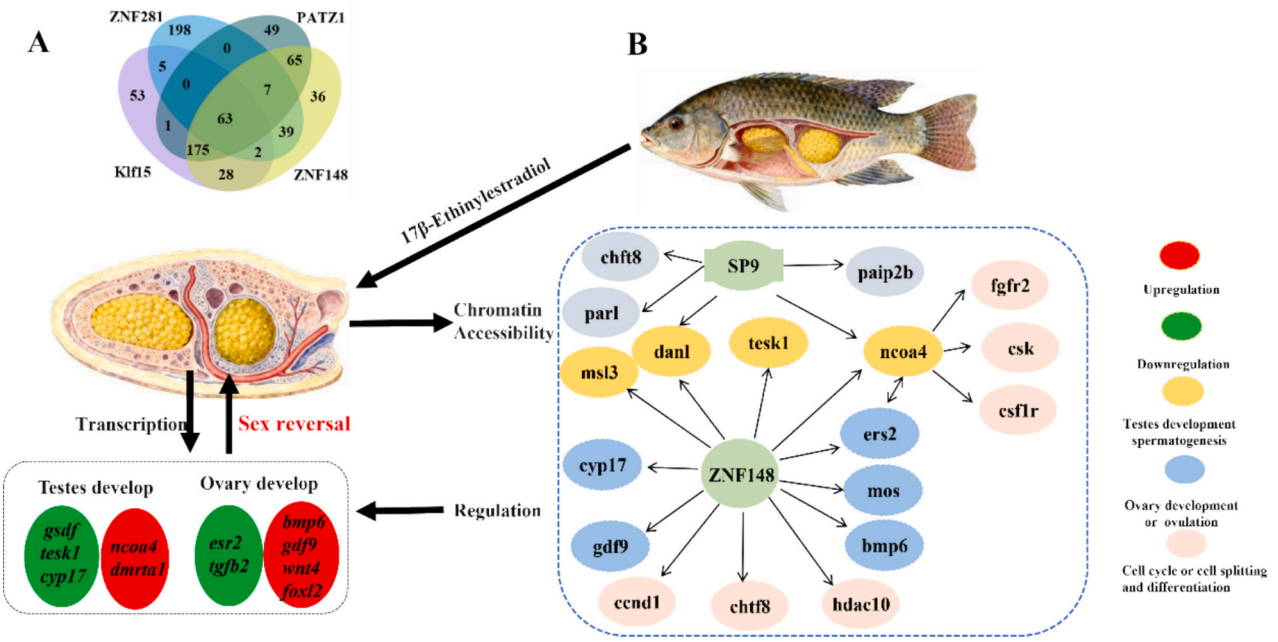


Fig. 5. Transcription Factor-Mediated Chromatin Accessibility and Regulatory Network in Sex Development.
A: Venn diagram analysis of transcription factors in CM VS S group ; B: Transcriptional Regulatory Networks of ZNF148 and SP9 in CM VS S Groups.

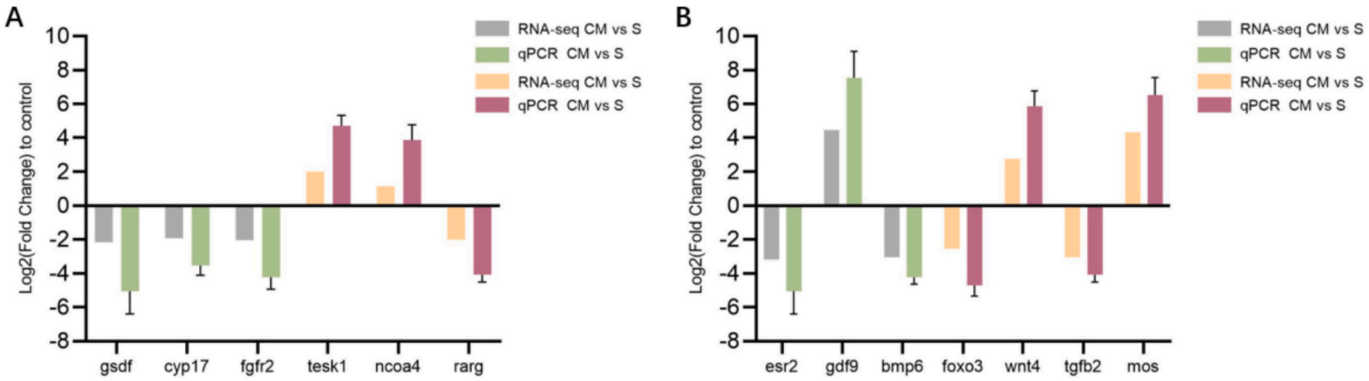


Fig. 6. qPCR Validation of Expression Profiles of Selected Genes Post Sex Reversal.
A: Regarding the Expression of Male Genes; B: Regarding the Expression of Female Genes.

4. Discussion

In this study, sex reversal was induced in male tilapia by feeding exogenous estrogen, transforming them into pseudo-female individuals, the proportion of females obtained in the hormone-treated group was 60%. Previous studies have shown that at appropriate concentrations, the sex reversal rate induced by EE2 can exceed 90% [13,19]. Therefore, we speculate that two primary factors contributed to this lower reversal rate: First, during feeding, some feed may not have been fully consumed by the fry, or hormones may have been washed away by water flow, resulting in an effective dose lower than the actual concentration. Second, uneven mixing of hormones with feed could have led to localized over-concentrations, triggering toxic effects and increased mortality, which further impaired sex reversal efficiency. Histological and hormonal analyses of the gonads revealed that the pseudo-female gonads did not fully develop into functionally normal ovaries; instead, they exhibited a delayed and dysfunctional state, albeit leaning toward the normal female phenotype. In terms of growth performance, the gonadal weight (GW), gonadosomatic index (GSI), and total visceral weight (TVW) of pseudo-females were comparable to those of normal males. However, within a one-year-old tilapia population, the GSI of normal females was significantly higher than that of pseudo-females. At equivalent body weights, the ovarian volume of pseudo-females was markedly smaller than that of normal females, with insufficient yolk deposition in the oocytes and a higher abundance of pale, early-stage or possibly degenerating oocytes present in the ovaries [20,21]. Hormonally, the estrogen levels in pseudo-females fell between those of CF and CM, showing no significant difference from normal females, whereas their androgen levels were significantly higher than those of normal females. These results indicate that although EE2-induced sex reversal can alter gonadal developmental fate, it does not achieve complete and healthy feminization.

The hormone-induced sex reversal process is irreversible, underscoring the importance of ensuring continued ovarian growth and development post-reversal. However, gene expression in pseudo-females exists in a “dysregulated state.” Transcriptomic data reveal that after sex reversal is completed, the gonads of pseudo-females begin developing toward ovaries, with certain genes associated with ovarian development and follicle formation (e.g., *wnt4*, *gdf9*, and *dnmt1*) showing upregulated expression in the ovaries [22–25], while some genes related to testis development (e.g., *gsdf*, *rarg*, and *hsd11b2*) exhibit downregulated trends [4,26,27]. This pattern aligns with the gene

expression levels observed during normal female gonadal development. Nevertheless, the gonadal transcriptome also revealed another expression pattern: some female-development-related genes (e.g., *tcf*, *esr2*) were downregulated, whereas certain male-development-related genes (e.g., *dmrta1*, *dmrta2*) were upregulated. This dysregulated gene expression profile was inferred to be responsible for the delayed ovarian development in pseudo-females. From a hormonal perspective, androgen levels in pseudo-females lie between those of normal females and normal males, but are significantly higher than in normal females, further supporting the observed dysregulation in gene expression.

To further elucidate the regulatory mechanisms underlying gonadal development in pseudo-females, chromatin accessibility in pseudo-female gonads was analyzed using ATAC-seq. Comparative analysis of differentially enriched transcription factors revealed that multiple transcription factors, including ZNF148, PRDM9, ZNF281, and SP9, regulate downstream genes. These factors all belong to the C2H2 zinc-finger protein family and exert strong regulatory effects on their downstream target genes. ZNF148 is a key regulator of biological processes such as cell proliferation, differentiation, and apoptosis [28,29], and it controls numerous genes involved in growth and development [28]. ZNF281 has been demonstrated to play a critical role in embryonic stem cell differentiation and tissue development [30,31]. PRDM9 primarily regulates chromosomal recombination processes and is closely associated with germ cell formation [32]. SP9 has been identified as a regulator of gene expression by recognizing specific DNA sequences, thereby influencing cell development and differentiation [33,34]. Notably, among the differentially enriched transcription factors, ZNF148 and SP9 are the most prominent, regulating genes such as *parl*, *paip2b*, *ncoa4*, *gsdf*, and *wnt4*. Studies have reported that *parl* and *paip2b* play certain roles in gonadal development in other animals. For example, *parl* promotes an increase in mitochondrial number and activity by maintaining mitochondrial structure and function in germ cells, thereby supplying energy for cellular growth and development [35,36]. Upregulation of *parl* expression can meet the energy demands during gonadal development while reducing the accumulation of reactive oxygen species (ROS). *paip2b* can interact with the poly(A)-binding protein (PABP), and research has shown that *paip2b* expression levels are extremely low in mouse testes and ovaries [37,38]. In contrast, the *paip2a* gene is expressed in reproductive tissues and is involved in regulating translation during late spermatogenesis in mice [39]. Although *parl* and *paip2b* were upregulated in pseudo-female gonads, this finding does not directly indicate a relationship with gonadal development and requires further validation. *Wnt4* has been clearly shown to play roles in both ovarian and testicular development in fish, including influencing folliculogenesis. *Ncoa4* can enhance androgen receptor transcriptional activity as well as promote the release of free iron for cellular utilization through ferritinophagy [40–42].

Through integrated analysis of ATAC-seq and RNA-seq data, we further analyzed and constructed a transcriptional regulatory network influencing gonadal development. The integrated results revealed that only a minimal number of DARs and DEGs showed associations in the CF vs S comparison, suggesting that at the epigenetic level the S group may closely resemble the CF group. In contrast, a substantial number of genes displayed DAR-DEG associations in the CM vs S comparison. GO and KEGG enrichment analyses of these co-upregulated genes showed enrichment in pathways related to binding and catalysis, apoptosis, homologous recombination, and spliceosome function. By integrating differential transcription factors and differentially expressed genes, we found that *ncoa4* was regulated by multiple transcription factors and serves as a key hub gene in the transcriptional network governed by ZNF148 and SP9. The upregulation of ncoa4 expression positively correlated with the expression of ZNF148 and SP9, and its genomic locus exhibited enhanced chromatin accessibility. As a hub gene, its upregulation may contribute to abnormal hormone receptor signaling in pseudo-females. Furthermore, *ncoa4* can induce ferroptosis, as demonstrated by extant research, dysregulation of *ncoa4* expression has been shown to disrupt normal physiological functions in the liver and brain tissues of fish, and induced corresponding pathological changes [43]; we infer that increased *ncoa4* expression promotes ferritinophagy, leading to elevated levels of free iron within cells, which could induce ferroptosis in granulosa cells [44]. This process may disrupt normal granulosa cell function and ultimately adversely affect oocyte development. Additionally, we observed an interaction between *ncoa4* and *esr2*, with *esr2* expression showing a negative correlation with *ncoa4*. Therefore, besides directly influencing ovarian development, *ncoa4* may also activate or suppress other gonadal development-related genes, contributing to delayed ovarian development and functional impairment in pseudo-females.

Although this study reveals potential mechanisms for delayed gonadal development in pseudo-female tilapia at the multi-omics level, it must be acknowledged that the experimental design has limitations. The absence two crucial control groups: 1) A genetically female (XX) group treated with estrogen, which would help distinguish whether the observed pseudo-female phenotype represents a specific outcome of sex reversal or a general effect of exogenous estrogen exposure, 2) A genetically male (XY) group that did not undergo sex reversal after estrogen treatment. Since this subgroup was not analyzed in the study, it remains unclear whether the incomplete feminization and developmental delay observed in pseudo-female fish (S group) resulted from exogenous hormones failing to fully override their inherent male developmental program, leading to an incomplete state of sex reversal. Obviously, the current results cannot definitively confirm that the observed molecular changes (e.g., altered chromatin accessibility and gene expression reprogramming) directly underlie the mechanism of "reversal maintenance". Instead, our results more accurately reflect the intermediate and dysregulated molecular profiles exhibited by pseudo-female gonads following hormone induction, compared to normal males and females. Consequently, future studies will incorporate these essential control groups and integrate functional experiments to definitively validate the precise roles of specific transcription factors and core genes (such as *ncoa4*) in maintaining sex reversal.

5. Conclusion

This study investigated the induction of sex reversal in male Nile tilapia using exogenous estrogens. It was revealed that the gonadal development of pseudo-female fish following sex reversal exhibits an intermediate state, which is more similar to that of female fish, at the epigenetic and transcriptomic levels. The findings indicate that the expression patterns of pseudo-female gonads do not fully resemble those of normal females. Instead, a regulatory network centered on transcription factors such as ZNF148 and SP9 modulates downstream genes (e. g. *ncoa4*, *esr2* and *gdf9*), maintaining gonadal development in an incompletely feminized state that results in delayed ovarian maturation. These changes collectively constitute the molecular basis of the incompletely feminized state and may be associated with the observed delay in ovarian maturation. These findings provide new clues for understanding the potential epigenetic and transcriptional mechanisms associated with gonadal development following sex reversal, thereby laying a crucial theoretical foundation for the optimization of sex control strategies in aquaculture.

CRediT authorship contribution statement

Ye Yuan: Writing – original draft, Validation, Investigation, Data curation. **Hongbo Xi:** Validation, Methodology, Data curation. **Shandong Chen:** Methodology, Investigation. **Zexun Zhou:** Methodology, Investigation. **Wenting Zhu:** Validation, Formal analysis. **Yunyun Liu:** Validation, Formal analysis. **Yongchun Li:** Validation, Formal analysis. **Zhongyuan Shen:** Validation, Supervision, Data curation. **Chongqing Wang:** Validation, Supervision, Data curation. **Jun Xiao:** Validation, Supervision, Data curation. **Shi Wang:** Validation, Supervision, Data

curation. **Wuhui Li:** Writing – review & editing, Supervision, Project administration, Funding acquisition, Data curation. **Shaojun Liu:** Writing – review & editing, Project administration, Funding acquisition.

Ethics approval

All the experimental procedures were conducted following the standards and ethical guidelines established by the Animal Ethical Review Committee of Hunan Normal University, Changsha, China.

Funding

This work was supported by the National Key research and Development Plan program of China (2022YFD2400801), the National Natural Science Foundation of China (32202906, 32293252, 32373119), the Science and Technology Innovation Program of Hunan Province (2024RC3282), Earmarked fund for Agriculture Research System of China (CARS–45), the Key Research and Development Program of Hunan Province of China (2024JK2034, 2025QY2004).

Declaration of competing interest

The authors declare there are no competing interests.

Acknowledgements

The authors thank each project for the funding and all the members of the laboratory for their careful experiments and valuable discussions.

Appendix A. Supplementary data

Supplementary data to this article can be found online at https://doi.org/10.1016/j.ygeno.2026.111230.

Data availability

Data will be made available on request.

References

[1] S. Cheng, M. Chi, S. Liu, J. Zheng, W. Jiang, X. Hang, M. Peng, F. Li, Study on hormone induction of the male parent and embryonic development, gonad differentiation, and growth of "all-female no.1" *Culter alburnus*, Heliyon 10 (2024) e33414, https://doi.org/10.1016/j.heliyon.2024.e33414.

[2] D. Liu, L. Gui, Y. Zhu, C. Xu, W. Zhou, M. Li, Chromosome-level assembly of male *Opsariichthys bidens* genome provides insights into the regulation of the GnRH Signaling pathway and genome evolution, Biol.-Basel 11 (2022) 1500, https://doi.org/10.3390/biology11101500.

[3] H. Liu, B. Guan, J. Xu, C. Hou, H. Tian, H. Chen, Genetic manipulation of sex ratio for the large-scale breeding of YY super-male and XY all-male yellow catfish (*Pelteobagrus fulvidraco (Richardson)*), Mar. Biotechnol. (N.Y.) 15 (2013) 321–328, https://doi.org/10.1007/s10126-012-9487-7.

[4] S.L.J. Lee, J.A. Horsfield, M.A. Black, K. Rutherford, A. Fisher, N.J. Gemmell, Histological and transcriptomic effects of 17α-methyltestosterone on zebrafish gonad development, BMC Genomics 18 (2017) 557, https://doi.org/10.1186/s12864-017-3915-z.

[5] M. Li, L. Sun, D. Wang, Roles of estrogens in fish sexual plasticity and sex differentiation, Gen. Comp. Endocrinol. 277 (2019) 9–16, https://doi.org/10.1016/j.ygcen.2018.11.015.

[6] G. Yoshizaki, S. Lee, Production of live fish derived from frozen germ cells via germ cell transplantation, Stem Cell Res. 29 (2018) 103–110, https://doi.org/10.1016/j.scr.2018.03.015.

[7] M.C. Adolfi, A.C. Carreira, L.W. Jesus, J. Bogerd, R.M. Funes, M. Schartl, M. C. Sogayar, M.I. Borella, Molecular cloning and expression analysis of dmrt1 and sox9 during gonad development and male reproductive cycle in the Lambari fish, *Astyanax altiparanae*, Reprod. Biol. Endocrinol. 13 (2015) 2, https://doi.org/10.1186/1477-7827-13-2.

[8] N. Yan, J. Hu, J. Li, J. Dong, C. Sun, X. Ye, Genomic organization and sexually dimorphic expression of the Dmrt1 gene in largemouth bass (*Micropterus salmoides*), Comp. Biochem. Physiol. B Biochem. Mol. Biol. 234 (2019) 68–77, https://doi.org/10.1016/j.cbpb.2019.05.005.

[9] Y. Guiguen, A. Fostier, F. Piferrer, C.-F. Chang, Ovarian aromatase and estrogens: a pivotal role for gonadal sex differentiation and sex change in fish, Gen. Comp. Endocrinol. 165 (2010) 352–366, https://doi.org/10.1016/j.ygcen.2009.03.002.

[10] M. Dussenne, J. Delcourt, P. Poncin, C.A. Cornil, E. Parmentier, Impact of temperature-induced sex reversal on behavior and sound production in Nile tilapia (*Oreochromis niloticus*), Horm. Behav. 142 (2022) 105173, https://doi.org/10.1016/j.yhbeh.2022.105173.

[11] Z.-G. Shen, H.-P. Wang, Molecular players involved in temperature-dependent sex determination and sex differentiation in Teleost fish, Genet. Sel. Evol. 46 (2014) 26, https://doi.org/10.1186/1297-9686-46-26.

[12] X. Wu, Y. Yang, C. Zhong, Y. Guo, T. Wei, S. Li, H. Lin, X. Liu, Integration of ATAC-seq and RNA-seq unravels chromatin accessibility during sex reversal in Orange-spotted grouper (*Epinephelus coioides*), Int. J. Mol. Sci. 21 (2020) 2800, https://doi.org/10.3390/ijms21082800.

[13] J. Pechsiri, A. Yakupitiyage, A comparative study of growth and feed utilization efficiency of sex-reversed diploid and triploid Nile tilapia, *Oreochromis niloticus L*, Aquac. Res. 36 (2005) 45–51, https://doi.org/10.1111/j.1365-2109.2004.01182.x.

[14] Y.-L. Sun, D.-N. Jiang, S. Zeng, C.-J. Hu, K. Ye, C. Yang, S.-J. Yang, M.-H. Li, D.-S. Wang, Screening and characterization of sex-linked DNA markers and marker-assisted selection in the Nile tilapia (*Oreochromis niloticus*), Aquaculture 433 (2014) 19–27, https://doi.org/10.1016/j.aquaculture.2014.05.035.

[15] J. Srijunngam, K. Wattanasirmkit, Histological structures of Nile Tilapia *Oreochromis niloticus* Linn. Ovary, Trop. Nat. His. 1 (2001) 53–59, https://doi.org/10.58837/tnh.1.1.102873.

[16] J.D. Buenrostro, B. Wu, H.Y. Chang, W.J. Greenleaf, ATAC-seq: a method for assaying chromatin accessibility genome-wide, Curr. Protoc. Mol. Biol. 109 (2015), https://doi.org/10.1002/0471142727.mb2129s109.

[17] Y. Yuan, Z. Zhou, S. Chen, Y. Liu, Y. Li, Y. Miao, S. Wang, Z. Shen, L. Zeng, J. Xiao, Q. Qin, W. Li, The expression of liver–gonadal axis genes reveals the long–term effects of exogenous estradiol on gonad development and liver function in *GIFT tilapia*, Reprod. Breed. 5 (2025) 11–20, https://doi.org/10.1016/j.repbre.2025.02.003.

[18] W. Li, Y. Miao, Z. Zhou, S. Wang, F. Hu, Z. Shen, L. Zeng, J. Hu, P. Wu, R. Zhao, M. Tao, C. Zhang, Q. Qin, S. Liu, The kiss2/kiss2r system directly modulates the activity of the pituitary gland in largemouth bass (*Micropterus salmoides*), Reprod. Breed. 3 (2023) 99–107, https://doi.org/10.1016/j.repbre.2023.06.003.

[19] O. Pacheco Passos Neto, A. Bezerra Dos Santos, J.R. Feitosa Silva, S. Mota, Alterations in the development and gonadal structure of Nile Tilapia (*Oreochromis niloticus*) exposed to natural and synthetic Estrogens, Water Air Soil Pollut. 232 (2021) 448, https://doi.org/10.1007/s11270-021-05375-x.

[20] N. Reyhanian Caspillo, K. Volkova, S. Hallgren, P.-E. Olsson, I. Porsch-Hällström, Short-term treatment of adult male zebrafish (*danio rerio*) with 17α-ethinyl estradiol affects the transcription of genes involved in development and male sex differentiation, Comp Biochem Physiol C Toxicol Pharmacol. 164 (2014) 35–42, https://doi.org/10.1016/j.cbpc.2014.04.003.

[21] H. Chen, S. Li, L. Xiao, Y. Zhang, G. Li, X. Liu, H. Lin, Wnt4 in protogynous hermaphroditic orange-spotted grouper (*Epinephelus coioides*): identification and expression, Comp. Biochem. Physiol. B Biochem. Mol. Biol. 183 (2015) 67–74, https://doi.org/10.1016/j.cbpb.2015.01.002.

[22] A.A. Mhanni, R.A. McGowan, Variations in DNA (cytosine-5)-methyltransferase-1 expression during oogenesis and early development of the zebrafish, Dev. Genes Evol. 212 (2002) 530–533, https://doi.org/10.1007/s00427-002-0275-7.

[23] H. Yu, Y. Wang, M. Wang, Y. Liu, J. Cheng, Q. Zhang, Growth differentiation factor 9 (gdf9) and bone morphogenetic protein 15 (bmp15) are potential intraovarian regulators of steroidogenesis in Japanese flounder (*Paralichthys olivaceus*), Gen. Comp. Endocrinol. 297 (2020) 113547, https://doi.org/10.1016/j.ygcen.2020.113547.

[24] X. Zhou, Y. He, X. Pan, H. Quan, B. He, Y. Li, G. Bai, N. Li, Z. Zhang, H. Zhang, J. Li, X. Yuan, DNMT1-mediated lncRNA IFFD controls the follicular development via targeting GLI1 by sponging miR-370, Cell Death Differ. 30 (2023) 576–588, https://doi.org/10.1038/s41418-022-01103-y.

[25] D.-N. Jiang, U.F. Mustapha, H.-J. Shi, Y.-Q. Huang, J.-X. Si-Tu, M. Wang, S.-P. Deng, H.-P. Chen, C.-X. Tian, C.-H. Zhu, M.-H. Li, G.-L. Li, Expression and transcriptional regulation of gsdf in spotted scat (*Scatophagus argus*), Comp. Biochem. Physiol. B Biochem. Mol. Biol. 233 (2019) 35–45, https://doi.org/10.1016/j.cbpb.2019.04.002.

[26] L. Ye, M. Zhu, J. Ju, H. Yang, Effects of dietary cholesterol regulation on spermatogenesis of *Gobiocypris rarus* rare minnow, Int. J. Mol. Sci. 24 (2023) 7492, https://doi.org/10.3390/ijms24087492.

[27] C.Z.Y. Zhang, G.G. Chen, P.B.S. Lai, Transcription factor ZBP-89 in cancer growth and apoptosis, Biochim. Biophys. Acta 1806 (2010) 36–41, https://doi.org/10.1016/j.bbcan.2010.03.002.

[28] A.K.Y. To, G.G. Chen, U.P.F. Chan, C. Ye, J.P. Yun, R.L.K. Ho, A. Tessier, J. L. Merchant, P.B.S. Lai, ZBP-89 enhances Bak expression and causes apoptosis in hepatocellular carcinoma cells, Biochim. Biophys. Acta 1813 (2011) 222–230, https://doi.org/10.1016/j.bbamcr.2010.09.005.

[29] L. Bai, J.L. Merchant, ZBP-89 promotes growth arrest through stabilization of p53, Mol. Cell. Biol. 21 (2001) 4670–4683, https://doi.org/10.1128/MCB.21.14.4670-4683.2001.

[30] T. Ishiuchi, H. Ohishi, T. Sato, S. Kamimura, M. Yorino, S. Abe, A. Suzuki, T. Wakayama, M. Suyama, H. Sasaki, Zfp281 shapes the transcriptome of trophoblast stem cells and is essential for placental development, Cell Rep. 27 (2019) 1742–1754.e6, https://doi.org/10.1016/j.celrep.2019.04.028.

[31] C.-J. Qin, P.-L. Bu, Q. Zhang, J.-T. Chen, Q.-Y. Li, J.-T. Liu, H.-C. Dong, X.-Q. Ren, ZNF281 regulates cell proliferation, migration and invasion in colorectal Cancer through Wnt/β-catenin signaling, Cell. Physiol. Biochem. 52 (2019) 1503–1516, https://doi.org/10.33594/000000104.

[32] K. Paigen, P.M. Petkov, PRDM9 and its role in genetic recombination, Trends Genet. 34 (2018) 291–300, https://doi.org/10.1016/j.tig.2017.12.017.
[33] Z. Liu, Z. Zhang, S. Lindtner, Z. Li, Z. Xu, S. Wei, Q. Liang, Y. Wen, G. Tao, Y. You, B. Chen, Y. Wang, J.L. Rubenstein, Z. Yang, Sp9 regulates medial ganglionic Eminence-derived cortical interneuron development, Cereb. Cortex 29 (2019) 2653–2667, https://doi.org/10.1093/cercor/bhy133.
[34] Q. Zhang, Y. Zhang, C. Wang, Z. Xu, Q. Liang, L. An, J. Li, Z. Liu, Y. You, M. He, Y. Mao, B. Chen, Z.-Q. Xiong, J.L. Rubenstein, Z. Yang, The zinc finger transcription factor Sp9 is required for the development of Striatopallidal projection neurons, Cell Rep. 16 (2016) 1431–1444, https://doi.org/10.1016/j.celrep.2016.06.090.
[35] E. Radaelli, C.-A. Assenmacher, J. Verrelle, E. Banerjee, F. Manero, S. Khiati, A. Girona, G. Lopez-Lluch, P. Navas, M. Spinazzi, Mitochondrial defects caused by PARL deficiency lead to arrested spermatogenesis and ferroptosis, ELife 12 (2026) e84710, https://doi.org/10.7554/eLife.84710.
[36] N. Zhou, Z. Liu, Z. Shi, L. Luo, M. Xuan, R. Zhu, K. Hu, X. Zhu, W. Xu, Y. Li, Z. Cao, Y. Zhang, PARL regulates porcine oocyte meiotic maturation by mediating mitochondrial activity, Theriogenology 235 (2025) 75–85, https://doi.org/10.1016/j.theriogenology.2025.01.005.
[37] J.J. Berlanga, A. Baass, N. Sonenberg, Regulation of poly(A) binding protein function in translation: characterization of the Paip2 homolog, Paip2B, RNA 12 (2006) 1556–1568, https://doi.org/10.1261/rna.106506.
[38] A. Yanagiya, G. Delbes, Y.V. Svitkin, B. Robaire, N. Sonenberg, The poly(A)-binding protein partner Paip2a controls translation during late spermiogenesis in mice, J. Clin. Invest. 120 (2010) 3389–3400, https://doi.org/10.1172/JCI43350.
[39] G. Delbes, A. Yanagiya, N. Sonenberg, B. Robaire, PABP interacting protein 2A (PAIP2A) regulates specific key proteins during spermiogenesis in the Mouse[1], Biol. Reprod. 86 (2012), https://doi.org/10.1095/biolreprod.111.092619.
[40] H.-Y. Kang, S. Yeh, N. Fujimoto, C. Chang, Cloning and characterization of human prostate coactivator ARA54, a novel protein that associates with the androgen receptor, J. Biol. Chem. 274 (1999) 8570–8576, https://doi.org/10.1074/jbc.274.13.8570.
[41] M.M. Rahman, H. Miyamoto, H. Takatera, S. Yeh, S. Altuwaijri, C. Chang, Reducing the agonist activity of antiandrogens by a dominant-negative androgen receptor coregulator ARA70 in prostate cancer cells, J. Biol. Chem. 278 (2003) 19619–19626, https://doi.org/10.1074/jbc.M210941200.
[42] S. Kuno, H. Fujita, Y. Tanaka, Y. Ogra, K. Iwai, Iron-induced NCOA4 condensation regulates ferritin fate and iron homeostasis, EMBO Rep. 23 (2022) e54278, https://doi.org/10.15252/embr.202154278.
[43] Y. Gao, H. Chen, H. Lian, X. Cai, L. Xie, R.G. Ahmed, X. Lin, H. Chen, W. Dong, The role of the ferroptosis pathway in the toxic mechanism of TCDD-induced liver damage in zebrafish, Comp. Biochem. Physiol. C Toxicol. Pharmaco. 295 (2025) 110213, https://doi.org/10.1016/j.cbpc.2025.110213.
[44] H. Wang, The role of granulosa cells in oocyte development and aging: mechanisms and therapeutic opportunities, Semin. Cell Dev. Biol. 171 (2025) 103614, https://doi.org/10.1016/j.semcdb.2025.103614.